

Connecting Energy Landscapes with Experimental Rates for Aminoacyl-tRNA Accommodation in the Ribosome

Paul C. Whitford,*,† José N. Onuchic,‡ and Karissa Y. Sanbonmatsu†

Theoretical Biology and Biophysics, Theoretical Division, Los Alamos National Laboratory, MS K710, Los Alamos, New Mexico 87545, and Center for Theoretical Biological Physics and Department of Physics, University of California, San Diego, 9500 Gilman Drive, La Jolla, California 92093

Received July 12, 2010; E-mail: whitford@lanl.gov

Abstract: Using explicit-solvent simulations of the 70S ribosome, the barrier-crossing attempt frequency was calculated for aminoacyl-tRNA elbow-accommodation. In seven individual trajectories (200-300 ns, each, for an aggregate time of 2.1 μ s), the relaxation time of tRNA structural fluctuations was determined to be \sim 10 ns, and the barrier-crossing attempt frequency of tRNA accommodation is $\sim 1-10 \ \mu s^{-1}$. These calculations provide a quantitative relationship between the free-energy barrier and experimentally measured rates of accommodation, which demonstrate that the free-energy barrier of elbow-accommodation is less than 15 k_BT , in vitro and in vivo.

Using explicit-solvent simulations of the 70S ribosome (3.2) million atoms, Table 1), we provide a quantitative relationship between free-energy profiles and experimentally determined kinetics for aminoacyl-tRNA (aa-tRNA) accommodation in the ribosome during tRNA selection (Figure 1). After initial selection, where the incoming aa-tRNA associates with the messenger RNA (mRNA) on the ribosome, accommodation displaces the encoded amino acid \sim 90 Å from outside of the ribosome to the peptidyltransferase center (PTC), where it is added into the nascent protein chain. When near-cognate aa-tRNA molecules successfully associate during initial selection, accommodation acts as a "kinetic proofreading" step,² where incorrect tRNAs are often rejected by the ribosome. This kinetic process is governed by the underlying thermodynamics, which have been the focus of experimental^{3,4} and theoretical^{5,6}

Simulations and theoretical models have the potential to provide a structural/energetic framework for interpreting rapid kinetic and single-molecule measurements, though comparison is rarely direct. Specifically, kinetics are measured in bulk experiments, while freeenergy profiles are far more difficult to obtain. In contrast, many molecular simulation methods are available to calculate the potential of mean force (i.e., the free energy along a specific degree of freedom) for biomolecular processes,8 while it is not feasible to directly measure rates. Consequently, calculations often focus on the fluctuations about particular configurations.⁹

To connect experimental accommodation kinetics and the freeenergy profile, one may use the relationship¹⁰

$$\frac{1}{k_{\rm a}} = \langle \tau_{\rm a} \rangle = \int_{\mathcal{Q}_{\rm A/T}}^{\mathcal{Q}_{\rm A/T}} \mathrm{d}Q \int_{\infty}^{\mathcal{Q}} \mathrm{d}Q' \, \frac{\exp[(G(Q) - G(Q'))/k_{\rm B}T]}{D(Q)} \tag{1}$$

Table 1. Summary of Diffusion Coefficient Calculations

conf	length (ns)	drift (Å/ns)	$\langle \Delta R^2 \rangle$ (Å ²)	$\langle \tau \rangle$ (ns)	$D_1 \ (\mu \text{m}^2/\text{s})$	D ₂ (μm ² /s)
A/T	301	1.5×10^{-2}	3.27	13.3	1.2	1.1
A/T	262	3.3×10^{-2}	5.79	35.4	0.8	0.9
A/T	260	-3.0×10^{-2}	4.07	17.3	1.2	0.6
A/T	261	4.5×10^{-4}	1.91	8.46	1.1	0.3
A/A	208	1.1×10^{-2}	2.76	19.7	0.7	1.0
A/A	205	9.4×10^{-3}	1.36	11.7	0.6	0.3
A/A	213	2.7×10^{-2}	1.47	7.64	1.0	0.2

where k_a is the rate of accommodation (referred to as k_5 elsewhere (ref 1)), $\langle \tau_a \rangle$ is the mean-first passage time, Q is the reaction coordinate, G(Q) is the Gibb's free energy, D(Q) is the diffusion in Q-space, and $Q_{A/T}$ and $Q_{A/A}$ are the values of Q that define the A/T and A/A configurations (Supporting Information). If G(Q) has a single barrier and D(Q) is constant (see Supporting Information), then eq 1 is approximated as

$$\frac{1}{k_{\rm a}} \approx \frac{1}{C_{\rm a}} \exp(\Delta G_{\rm TSE}/k_{\rm B}T) \tag{2}$$

where $\Delta G_{ ext{TSE}}$ is the difference in the free energy of the A/T ensemble and the transition state ensemble (TSE) and C_a is the barrier-crossing attempt frequency. While this general relationship relates kinetic rates and the free-energy profile, the attempt frequency C_a is process-specific. The barrier-crossing attempt frequency is determined by the diffusion coefficient and the distance between the end points (both in Q-space).

While accommodation is likely a multistep process,⁶ here the discussion is restricted to tRNA elbow-accommodation (measured by R_{elbow} , Figure 1), for comparison to single-molecule data.^{6,11} To determine the attempt frequency, we calculated $D_{\rm elbow}(R_{\rm elbow})$ (diffusion coefficient in $R_{\rm elbow}$) from explicit-solvent simulations, set eqs 1 and 2 equal to each other, and numerically integrated eq 1. Since free-energy profiles of accommodation have not previously been determined, the functional form of $G(R_{elbow})$ was varied to establish robustness of the results (Supporting Information).

Simulations of the 70S ribosome, fully solvated with physiological concentrations of ions, were performed (Table 1). The diffusion coefficient in elbow distance, Delbow, was determined using two different strategies. The first approach was to use the quasi-harmonic approximation to the dynamics, as employed in protein folding studies, ¹² where $D_{\text{elbow}} = \langle \Delta R_{\text{elbow}}^2 \rangle / (2\tau_{\text{elbow}})$. $\langle \Delta R_{\text{elbow}}^2 \rangle$ is the meansquared fluctuations in distance, and $au_{
m elbow}$ is the decay time associated with the fluctuations (Figure 2C-E). With this procedure, D_{elbow} (labeled D_1 in Table 1) for the A/T and A/A ensembles (Supporting Information) was 1.1 ± 0.1 and $0.8 \pm 0.1 \,\mu\text{m}^2/\text{s}$. The second strategy employed¹³ $D_{\text{elbow}} = \lim_{t\to\infty} (\partial/\partial t) \langle |R_{\text{elbow}}(t)| R_{\rm elbow}(0)|^2$ /2. The mean-squared displacement is linear from 10 to

Los Alamos National Laboratory

^{*} University of California, San Diego.

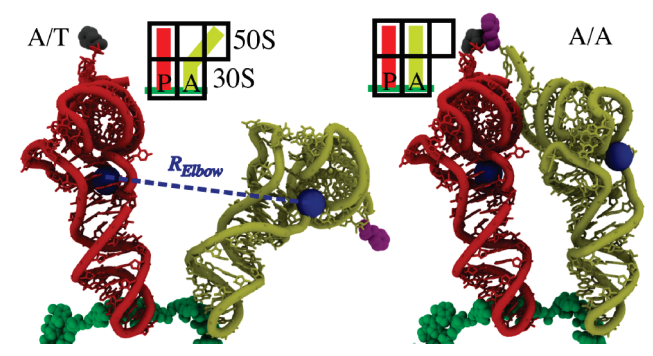


Figure 1. Structural representation of aa-tRNA (yellow), p-tRNA (red), mRNA (green), and the associated amino acids (gray, purple) in the partially bound A/T conformation (left) and fully bound A/A conformation (right). Elbow-accommodation is indicated by R_{elbow} , the distance between the O3' atoms of U8 on p-tRNA and U47 on aa-tRNA (blue spheres).

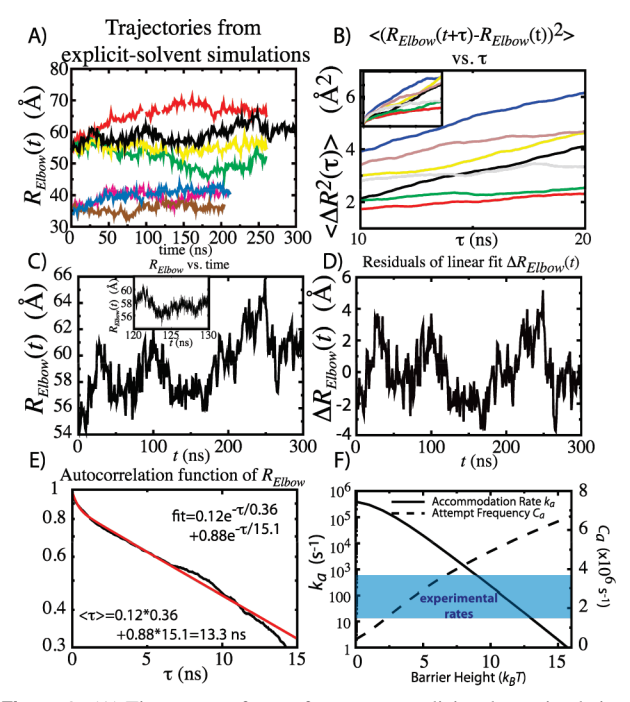


Figure 2. (A) Time traces of R_{elbow} from seven explicit-solvent simulations. (B) Mean-squared displacement $\langle \Delta R_{\rm elbow}^2(\tau) \rangle$ as a function of time delay τ . $D_{\rm elbow}$ was estimated by the slope between 10 and 20 ns. Inset shows $\langle \Delta R_{\rm elbow}^2(\tau) \rangle$ for $\tau = 0-30$ ns. (C) 300 ns trajectory, displayed at 1 ns intervals. Inset shows subset at 5 ps intervals. (D) Dispersion and relaxations calculated from the residuals of linear fit (slopes in Table 1), ΔR_{elbow} . (E) Autocorrelation function of ΔR_{elbow} fitted to the sum of two exponentials (Supporting Information). D_{elbow} was calculated from the average decay time $\langle \tau \rangle$. (F) Accommodation rate k_a and attempt frequency C_a , for $D_{\text{elbow}} = 1.1$ µs²/s, versus the free-energy barrier height. Range of experimentally determined rates shaded in blue.

20 ns, yielding diffusion coefficients (labeled D_2 in Table 1) of 0.8 \pm 0.2 μ m²/s (A/T) and 0.5 \pm 0.2 μ m²/s (A/A). In the case of infinite sampling, the two approaches should yield identical values. Here, the two values of $D_{\rm elbow}$ are within the statistical uncertainty. In solution, the diffusion coefficient of a ternary complex has been estimated at $0.3-2.5 \,\mu\text{m}^2/\text{s}$. Since diffusion is determined by the degree of roughness in the landscape, the striking similarity between the diffusion in solution and inside the ribosome suggests there is a low degree of roughness in the energy landscape of accommodation.

Figure 2F shows the accommodation rate k_a as a function of barrier height, obtained through numerical integration of eq 1 (Supporting Information), with $D_{\text{elbow}} = 1.1 \ \mu\text{m}^2/\text{s}$. The attempt frequency C_a was also calculated as a function of barrier height.

The attempt frequency is proportional to the curvature of the initial and final basins. 15 Since the curvature of the basins increases with increasing barrier height (see Supporting Information), the observed increase in attempt frequency (Figure 2F) is expected.

Depending on the barrier height and functional form (Supporting Information), the attempt frequency for elbow-accommodation is $\sim 1-8 \,\mu s^{-1}$, which is in the same range of values as for small RNA $(0.1-1.6 \ \mu s^{-1})^{16}$ and protein $(0.1-20 \ \mu s^{-1})^{15}$ folding.

Here, we employed $D_{\text{elbow}}=1.1 \,\mu\text{m}^2/\text{s}$, which is our upper-bound estimate. Accordingly, the rate for a given barrier height, and the barrier height for a given rate, should be considered upper bounds. Bulk kinetic experiments have reported the rate of full accommodation to range from tens to hundreds per second^{3,4} (shaded blue in Figure 2F). These rates suggest an $\sim 9-13 k_B T$ barrier height (this assumes elbow accommodation is rate limiting during accommodation). Since accommodation is not barrierless, targeting its TSE^{6,11} is a viable approach for gaining quantitative control of translation. Finally, this study establishes the conversion between kinetics and free-energy profiles. With this conversion, it is now possible to validate the details of the free-energy profiles obtained from smFRET and simulations through comparison with kinetic data for large-scale conformational rearrangements in the ribosome.

Acknowledgment. This work was supported by the LANL LDRD program, NIH Grant R01-GM072686, the Center for Theoretical Biological Physics, sponsored by the NSF (Grant PHY-0822283), with additional support from NSF-MCB-0543906. We are also grateful for computing time on the NMCAC Encanto Supercomputer and the LANL Roadrunner Supercomputer.

Supporting Information Available: Simulation details and description of rate calculations. This material is available free of charge via the Internet at http://pubs.acs.org.

References

- (1) Rodnina, M. V.; Wintermeyer, W. Annu. Rev. Biochem. 2001, 70, 415-
- Hopfield, J. J. Proc. Natl. Acad. Sci. U.S.A. 1974, 71, 4135-4139.
- Gromadski, K. B.; Rodnina, M. V. Mol. Cell 2004, 13, 191-200.
- Johansson, M.; Bouakaz, E.; Lovmar, M.; Ehrenberg, M. Mol. Cell 2008, 30, 589-598.
- Sanbonmatsu, K. Y.; Joseph, S.; Tung, C.-S. Proc. Natl. Acad. Sci. U.S.A.
- 2005, 102, 15854–15859.
 Whitford, P. C.; Geggier, P.; Altman, R.; Blanchard, S. C.; Onuchic, J. N.; Sanbonmatsu, K. Y. RNA 2010, 16, 1196–1204.
 Schuler, B.; Lipman, E. A.; Eaton, W. A. Nature 2002, 419, 743–747.
- (a) Garcia, A. E.; Paschek, D. *J. Am. Chem. Soc.* **2008**, *130*, 815–817. (b) Vaiana, A.; Sanbonmatsu, K. Y. *J. Mol. Biol.* **2009**, *386*, 648–661. (c) McDowell, S. E.; Špačková, N.; Šponer, J.; Walter, N. G. *Biopolymers* **2007**, 85, 169–184. (d) Hansson, T.; Oosenbrink, C.; van Gunsteren, W. F. *Curr. Opin. Struct. Biol.* **2002**, *12*, 190–196.
- (a) Besseová, I.; Réblová, K.; Leontis, N. B.; Šponer, J. *Nucleic Acids Res.* 2010, doi: 10.1093/nar/gkq414. (b) Romanowska, J.; Setny, P.; Trylska, J. *J. Phys. Chem. B* **2008**, *112*, 15227–15243. (c) Trabuco, L. G.; Harrison, C. B.; Schreiner, E.; Schulten, K. Structure 2010, 18, 627-637. (d) Petrone, P. M.; Snow, C. D.; Lucent, D.; Pande, V. S. *Proc. Natl. Acad. Sci. U.S.A.* **2008**, *105*, 16549–16554. (e) Tama, F.; Valle, M.; Frank, J.; Brooks, C. L. Proc. Natl. Acad. Sci. USA. 2003, 100, 9319–9323.
- (10) (a) Bryngelson, J. D.; Wolynes, P. G. J. Phys. Chem. 1989, 93, 6902–6915. (b) Zwanzig, R. Proc. Natl. Acad. Sci. U.S.A. 1988, 85, 2029.
 (11) (a) Marshall, R. A.; Aitken, C. E.; Dorywalska, M.; Puglisi, J. D. Annu. Rev. Biochem. 2008, 77, 177–203. (b) Geggier, P.; Dave, R.; Feldman, M. B.; Terry, D. S.; Altman, R. B.; Munro, J. B.; Blanchard, S. C. J. Mol. Biol. 2019, 2015, 2015. Biol. 2010, 399, 576-595.
- (12) (a) Chahine, J.; Oliveira, R. J.; Leite, V. B. P.; Wang, J. Proc. Natl. Acad. Sci. U.S.A. 2007, 104, 14646–14651. (b) Socci, N. D.; Onuchic, J. N.; Wolynes, P. G. J. Chem. Phys. 1996, 104, 5860–5868.
- (13) Yeh, I.-C.; Hummer, G. Biophys. J. 2004, 86, 681–889.
 (14) Zhang, G.; Fedyunin, I.; Miekley, O.; Valleriani, A.; Moura, A.; Ignatova, Z. Nucleic Acids Res. 2010, 384778-4787.
- (15) (a) Kubelka, J.; Hofrichter, J.; Eaton, W. A. Curr. Opin. Struct. Biol. 2004, 14, 76-78. (b) Tang, J.; Kang, S.-G.; Saven, J. G.; Gai, F. J. Mol. Biol. **2009**, 389, 90–102.
- (16) Thirumalai, D.; Hyeon, C. Biochemistry 2005, 13, 4957-4970.

JA1061399